

AN INTERDISCIPLINARY OPTIMIZATION APPROACH FOR CUTTING ATTRIBUTES OF LASER BEAM MACHINING

LAKSHMI CHAITANYA MADDILA ¹, AVINASH GUDIMETLA ²,
SUNIL RAJ MUSINADA ³ and SRIKANTH SRIMANTHULA ⁴

^{1,2,3,4}, Department of Mechanical Engineering, Pragati Engineering College, Surampalem AP, India.
Email: ¹maddilalakshmichaitanya@gmail.com

Abstract

To improve and optimize the responses of a machining process, the choice of input machining control parameters is to be set at an optimal value. As such one has to take up experimental methods, which are cumbersome, time-consuming, costly, and at times not feasible. During such situations, optimization techniques like Genetic Algorithm (GA) can be used as they provide a cost-effective method for solving such complex problems. Laser beam cutting is a non-traditional machining process that can be successfully used for the cutting of conductive and nonconductive difficult-to-cut advanced engineering materials such as reflective metals and composites. Al7075 aluminum alloy as matrix and silicon carbide (SiC) as reinforcement is a widely used material having potential applications in aircraft and space industries because of its lower weight-to-strength ratio. Considering these, an attempt is made for the optimization of Nd: YAG Laser beam cutting of Al7075/10%/SiCp metal matrix composite. In this research work, the desired responses are minimum kerf width and kerf deviation. The process parameters considered are pulse power, pulse frequency, assist gas pressure and pulse width. Experiments are conducted using a central composite design and the mathematical models correlating the desired responses and the control parameters are established using Response Surface Methodology (RSM). These models give the factor effects of the individual process parameters. Finally, GA is applied to search the optimal machining parameters.

Keywords: Laser cutting, Nd: YAG, kerf width, kerf deviation, Response Surface Methodology, Genetic Algorithm.

1. INTRODUCTION

Lasers are well-recognized and a very flexible tool for producing various micro-structures in this modern era, especially in the amelioration of engineering materials [1]. Laser Beam Machining (LBM) is one of the advanced non-conventional machining processes that is contemporarily used for shaping almost a whole range of engineering materials where complex contours demand precise, fast, and force-free processing. Besides marking, drilling, and welding applications, cutting is the most intermittently applied LBM process. The big benefit of laser beam cutting (LBC) is the localized laser energy input providing small focal diameters, small kerf widths, high feed rate, and minimal heat input

The laser cutting process works in principle by focusing a laser beam on a workpiece that needs processing. Laser beam cutting is a non-contact type; thermal energy-based advanced machining process works in principle by focusing a laser beam on a workpiece that needs processing. Due to the focused laser beam, the workpiece is heated up in the small area around it. This causes the melting of the material. The molten material is ejected through the bottom of the workpiece due to the pressure of a cutting assist gas. The area from where the material is removed is called the cut kerf (Figure 1). A high-pressure co-axial assist gas is supplied with

the nozzle to remove the molten metal from the melting pool. The effectiveness of the laser cutting process depends upon the thermal properties and to some extent optical properties, rather than mechanical properties of the material to be cut. Therefore, materials that exhibit a high degree of brittleness or hardness and have favorable thermal properties such as low thermal diffusivity and conductivity are well suited for laser cutting. The most imperative performance measures in LBC are kerf width (k_w) and kerf deviation (k_d) [2]. Kerf width indicates the degree of accuracy and kerf deviation measured along the length of the cut. These performance measures are governed by input-cutting variables such as laser power, pulse frequency, type of assist gas, and gas pressure. Laser cutting is a vastly entangled schema at which point an ample number of parameters need to be literally forbidden in unison, hence empirical optimization of the process is exorbitant and time expending. Therefore, a productive method is needed to arbitrate the optimal machining parameters.

The material used for experiments is silicon carbide (SiC_p) reinforced aluminum metal matrix composite which are the most advantageous engineering material due to its properties such as low weight, heat-resistant, wear-resistant, and low cost [3]. However, the full potential of this composite material is hindered by the high manufacturing cost together with the problems undergone in machining SiC_p -reinforced aluminum MMCs using conventional processes resulting in excessive tool wear owing to the hard, brittle and abrasive nature of this material [4]. Different aspects of the machining of this composite are investigated by researchers [5]. Very sparse research work is available in the field of LBC of this composite. Therefore, it is imperative to develop a suitable technology guideline for optimum and effective machining of Al/ SiC_p MMC.

Process modeling and optimization is one of the most benchmarked areas of machining as this results in the diminution of production cost and improvement of product quality. However, wherefore the intricate, fused, and non-linear nature of the input–output variables of machining processes, experimental optimization of any machining process is inflated and time-devouring. Abruptly, existing cogent models and analyses cannot impart judicious process foresight for better quality control and higher throughput owing to the highly convoluted interactions between process parameters.

The present work formulates LBC explicitly as an optimization problem for the determination of the optimal machining conditions involving the minimization of kerf width and kerf deviation during Nd: YAG laser cutting of Al7075/10%/ SiC_p metal matrix composite. The mathematical models for the kerf width and kerf deviation are developed through the response surface methodology (RSM). Later RSM models are coupled with GA to find the optimum process parameter values.

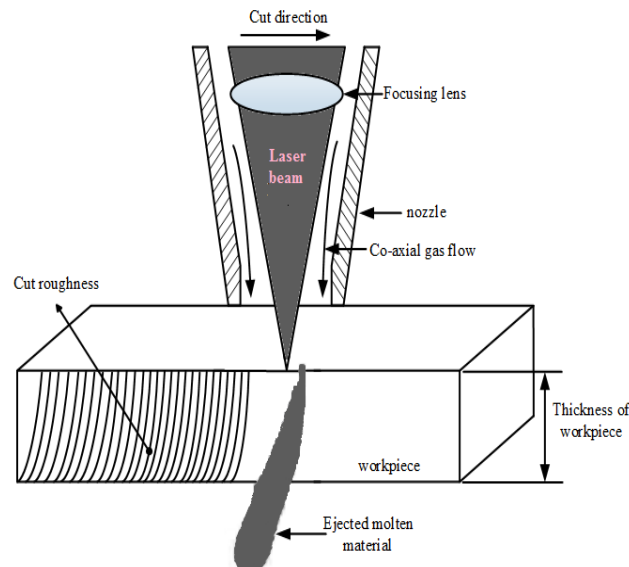


Figure 1: Principle of laser beam cutting process

2. LITERATURE REVIEW

The most primarily used lasers are continuous wave (CW), CO₂ and pulsed Nd: YAG [6]. Various researchers [7-8] have put up the efforts for cutting of composite by CO₂ laser/ND: YAG laser approaches. Pulsed Nd: YAG laser cutting becomes an exemplary cutting process because of high laser beam potential, low mean beam power, good focusing features, and narrow HAZ [9]. The quality of cut mainly depends upon the combination of process parameters such as laser power, type and pressure of assist gas, cutting speed, sheet material thickness and its chemical composition. Researchers [10-11] have investigated the effect of laser cutting parameters on cut geometry and cut surface quality. To analyze the effect of process parameters on kerf width and kerf deviation, Ghany and Newishy (2005) [12] during his study found that kerf width increases with the increase of laser power and decreasing the cutting speed and type of gas and pressure during experimental study of Nd: YAG laser cutting of 1.2mm thick austenitic stainless steel sheet. They also found that kerf width decreases with the increases of pulse frequency. The optimal operating parameters are very difficult to be controlled and greatly complicated due to the influence of operating parameters on the performance characteristics. In such complex and multi-variate systems, the relationship between factors is unclear. Optimization of the machining process first requires a mathematical model to be established to correlate the desired response and the process control parameters. Thereafter an optimization technique is applied to find optimal setting of the control parameters to derive the desired responses. Dubey and Yadava [13] have performed the optimization of laser beam cutting process of thin sheets (0.5 mm thick) of magnetic material using hybrid Taguchi method and response surface method. The same authors [14] have performed the multi-objective optimization of kerf quality using two kerf qualities such as kerf deviation and kerf width using Taguchi quality loss function for pulsed Nd: YAG laser cutting of thin sheet

of aluminium alloy. Rao and Yadava [15] presented a hybrid optimization approach (TM-GRA) for the determination of optimum laser cutting parameters which minimize the kerf width and kerf deviation during Nd: YAG pulsed laser cutting of nickel –based super alloy.

Dubey and Yadava [16] presented a hybrid optimization approach (TM-PCA) for multi-objective optimization for the determination of optimum laser cutting parameters which minimize the kerf width and kerf deviation during Nd: YAG pulsed laser cutting of nickel –based super alloy.

Sharma et al. [17] conducted experiments based on the Taguchi quality design concept for parameter optimization of the kerf quality characteristics during pulsed Nd: YAG laser cutting of nickel based super alloy thin sheet. Sivarao et al. [18] have used ANFIS modeling for laser cutting in order to analyze the effect of input process parameters such as standoff distance, focal distance, gas pressure, laser power, cutting speed, frequency and duty cycle on the output parameters kerf width. Also in the recent past, pulsed Nd: YAG laser cutting has been widely used for precision cutting of thin sheets of materials like mild steel[19], stainless steel [19,12], nickel based super alloys [10,16], Al/Li/SiC Metal Matrix Composites[20] etc.

3. CRITIQUE ON THE LITERATURE SURVEY

From the literature, it is pragmatic that most of the experimental work [19, 12, 10, 16] on laser cutting is on kerf quality based on kerf width, while minimization of that ensures a narrow kerf. But minimization of kerf unevenness or kerf deviation along length of cut is also an important quality characteristic for obtaining a uniform kerf.

Authors have found in [14] where kerf deviation parameter has been taken care off. The literature outline affirms that the potential of the laser cutting of kerf width rely upon mainly on the laser power, pulse frequency, cutting speed and focus positions and kerf width increases in relation with power. Also literature validitates that appropriate efforts were dedicated to evaluate the most proven models for k_w and k_d .

These feasible models were employed as objective functions and were optimized to obtain the manufacturing conditions for the required k_w and k_d . Also the literature shows that the imperious modeling and optimization tools exerted up to now have been are primarily Taguchi-based regression analysis, ANFIS.

To assert the objective function and constraints as functions of the decision variables, the consistency and liability of ascertaining the planetary optimum solution confide in the type of modeling technique used [21]. Therefore, effective, efficient, and profitable implementation of the LBC process coerces an authentic modeling and optimization method.

In the utmost accustomed deterministic applications such as multiple regressions, a prediction model has to be determined in earlier and a set of coefficients has to be found. Also predicting system modeled by ANFIS cannot be used for real trade practices as large amount of training data might be required to develop an accurate system, depending always on the research study.

4. PROPOSED METHODOLOGY

In this paper, a unique way of modeling kerf width and kerf deviation using RSM is perceived. RSM is selected to map the experiments with a reduced number of trial runs to effectuate optimum responses. The discrete feature of RSM used extensively in the industrial world is used to examine and characterize problems in which input variables influence some performance aspect of the product or process. This performance measure, or sometimes quality characteristic, is called the response. More details of this methodology are discussed in Section 5. The models developed by RSM are subsequently used for optimization. In the existing work, the optimization problem of LBC is framed as an optimization problem for the determination of the optimal machining conditions between kw and kd. It can be noted that the classical optimization methods (weighted sum methods, goal programming, min-max methods, etc.) are not suitable to solve problems where the formulated objective functions and constraints are very complicated and implicit functions of the decision variables [22]. Unlike conventional optimization techniques, GA is a powerful tool in experimental optimization, even when the experimenter does not have a model for the process. The GA is an optimization algorithm and objective function does not need to be differentiable. This allows the algorithm to be used in solving difficult problems, such as multi model, discontinuous or noisy systems. The great advantage of the GA is that it doesn't need to generate models and forbidden or unreachable combination of the factor settings can be simply put aside with another run of the program [23]. Hence, considering these advantages of GA, an attempt has been made to optimize the LBC process in this research paper using this technique.

5. MODELLING USING RSM

The theory of response surface methodology (RSM) was introduced by Box and Wilson [24] to develop the empirical models of complex processes. These models were used to represent the output characteristics (responses). Hill and Hunter [25] reviewed the earlier work on RSM. RSM is a combination of mathematical and statistical techniques useful for modeling and analyzing the problem in which several independent variables influence a dependent variable or response [26]. The successful application of RSM relies on the identification of suitable approximation for the function. The necessary data for building the response models are generally collected by an experimental design [23]. One of the most popular of classes of the RSM designs is the central composite design, or CCD.

The general second-order polynomial response is described as follows:

$$Y = y - \gamma = a_0 + \sum_{p=1}^k a_p x_p + \sum_{p=1}^k a_{pp} x_p^2 + \sum_{p < q} a_{pq} x_p x_q \quad (1)$$

where Y is the estimated response on a logarithmic scale, y is the measured response on a logarithmic scale, x_p is the logarithmic transformation of the p^{th} variable, k represents the number of input variables, γ is the experimental random error which is normally distributed with mean equal to 0, and a values are the estimates of the corresponding parameters which are estimated by the method of least squares. In the above equation, the second, the third, and the

fourth term represent the linear, the second-order, and the interactive effects of the input variables, respectively.

6. OPTIMIZATION USING GA

The concept of genetic algorithms (GA) was developed by Holland in the 1960s and 1970s [27]. The genetic algorithm is a probabilistic technique that uses a population of designs rather than a single design at a time. It is analogous to natural selection in the evolution of living organisms in that the fittest members in the population have a better chance to survive, reproduce and thus transfer their genetic material to the successive generations.

The initial population is produced by a set of arbitrarily generated members. Each generation comprises of members whose constituents are the individual design variables that differentiate a design and these are entrenched in a binary string. Each member is estimated using the objective function and is assigned a fitness value, which is a sign of the presentation of the member proportionate to the other members in the population. A biased selection depending on the fitness value, decides which members are to be used for producing the next generation. The chosen strings are the parents for the next generation, which emerges from the use of two genetic operators namely crossover and mutation. These operators give a random displacement to the parent population and engender a new population of designs.

The crossover operator takes two parent strings, separates them at a random location and swaps the sub-strings so formed. A probability of crossover decides even if a crossover should be performed.

The mutation operator inverts a bit in the string relying upon on the probability of mutation. The new strings developed are measured and the iteration lasts until a maximum number of generations have been reached or until a user defined termination criterion has been met. Figure 2 shows the sequence of steps in a basic genetic algorithm. The control parameters that have to be initially stated are the population size, the crossover and mutation probabilities, the maximum number of generations and the termination criterion [27].

7. EXPERIMENTAL DETAILS

The investigation of experiments was enforced with an optical fibre delivered pulsed Nd: YAG laser beam system (Model: JK300D) fabricated by GSI Lumonics and delivering maximum peak power of 16 kW. The laser beam was transmitted via a 300- μ m diameter step-indexed optical fibre to the cutting head, which was mounted over a six-axis robot (Model: IRB1410). The robot has the weight of 225 kg, handling competence of 5 kg at the wrist and a large working space. The cutting head was furnished with an automatic standoff adjusting servomotor and electrostatic sensor. The sensor is integrated to the robot control. The experimental set up of robotic laser cutting process was shown in Figure 2. The output laser beam was focused by a BK7 plano-convex lens whose focal distance was 116 mm. The fixed conditions at which the experiments were conducted were listed in Table 1. Economic grade Aluminum alloy 7075 and SiC granulars of particle size 50 μ m were selected for the present

work and the chemical composition was given in Table 2. The work material used for the current analysis was Al7075/10%SiCp composite with dimensions of 90 mm in length and 2 mm in thickness and the composite was fabricated by the stir casting method.

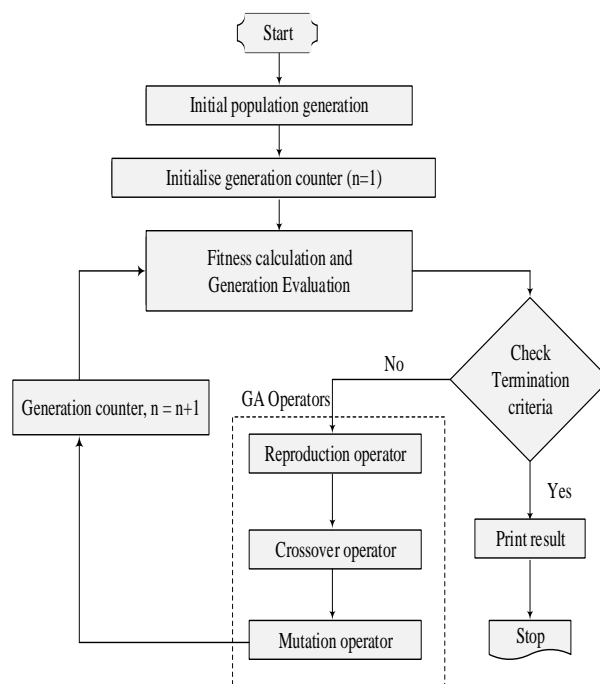


Figure 2: General Procedure for GA

Because of the large number of independent parameters that control the laser cutting process, some preliminary experiments were conducted in order to determine which parameters should be considered for optimization. The four control variables, viz. Pulse Power (PP), Pulse Frequency (PF), Assist Gas pressure (GP) and Pulse width (PW) each at five levels were chosen. The different levels of the parameters used in the experimentation are shown in Table 3.

It was decided to use a five-level test for each factor since the determined factors were multi-level variables whose outcome effects were not linearly related. The levels were fixed based on detailed preliminary experiments. The two quality characteristics analyzed were kerf width and kerf deviation (Figure 4). Two cuts each of 10mm length were obtained in each experimental run for all specimens. The kerf width was measured using an optical measuring microscope, OLYMPUS STM6. The kerf deviation in each experimental run is obtained by taking the mathematical average of the difference run by taking the mathematical average of the difference between maximum and minimum top kerf widths for two cuts measured along the length (Figure 4). The kerf width in each experimental run is obtained by taking a mathematical average of the top kerf widths of two cuts where the kerf width of each cut is the average of top kerf widths measured at four places along the length of the cut. The experiments

were planned implementing second-order central composite rotatable design (CCD) for the design of experiments (DOE), which helps to minimize the number of experiments. The results for 30 experiments after laser beam cutting which were evaluated as stated earlier on two performance measures were shown in Table 4.

8. DEVELOPMENT OF EMPIRICAL MODELS BASED ON RSM

Based on the CCD, experiments were executed to develop empirical models for kerf width (k_w) and kerf deviation (k_d) in terms of the four input variables. Using CCD it is liable to fit models up to the second order along with the quadratic terms. Design Expert 7.1, [28] software was used for analyzing the experimental results. Values of various regression statistics were compared to identify the best fit model. The need in developing the mathematical relationships was to correlate the machining responses to the cutting parameters thereby facilitating the optimization of the machining process. The statistical models based on the second-order polynomial equations formulated for k_w and k_d using the experimental details were given below:

$$\begin{aligned} \text{Kerf width} = & +0.37 + 0.030X_1 + 0.001034X_2 + 0.011X_3 - 0.007014X_4 - 0.001062X_1X_2 + \\ & 0.001391X_1X_3 + 0.005543X_1X_4 + 0.018X_2X_3 + 0.012X_2X_4 - 0.032X_3X_4 - 0.036X_1^2 - \\ & 0.052X_2^2 - 0.032X_3^2 - \\ & 0.034X_4^2 \end{aligned} \quad (2)$$

$$\begin{aligned} \text{Kerf deviation} = & +0.019 - 0.0015X_1 + 0.0054X_2 + 0.003050X_3 - 0.001517X_4 + \\ & 0.019X_1X_2 - 0.016X_1X_3 + 0.0068X_1X_4 - 0.0012X_2X_3 + 0.0056X_2X_4 - 0.0075X_3X_4 + \\ & 0.0050X_1^2 - 0.003692X_2^2 + 0.020X_3^2 + \\ & 0.004458X_4^2 \end{aligned} \quad (3)$$

The analysis of variance (ANOVA) was used to validate the competence of the developed models. Table 5 demonstrates the ANOVA for the kerf width. The P (significance) value for the model was lower than 0.05 (i.e. at 95% confidence level) indicates that the model is well thought-out to be statistically significant i.e. the differences among the means were meaningful and not the result of random chance [29]. Similar analysis was conceded out for the kerf deviation and was given in Table 6. The normal probability plots of the residuals for the output responses were shown in Figures 5 and 6. An analysis on these plots affirms that the residuals were located on a straight line, which means that the errors were distributed consistently and the regression models were proportionately well fitted with the observed values. To check whether the fitted models actually interpret the experimental data, the multiple regression coefficients (R^2) were computed. The multiple regression coefficients (R^2) for kerf width and kerf deviation were found to be 0.9733 and 0.9759 respectively. This shows that the second-order model can justify the variation in the kerf width and kerf deviation up to the measure of 97.33% and 97.59%, respectively. It can be said that the second-order models were adequate in representing the process on the basis of these values of the multiple regression coefficients.

Table 1: Cutting conditions

1 Work piece material	: Al 7075/10% SiCp
2 Material Dimensions	: 90 mm X 30 mm X 2 mm
3 Power of laser	: 16W
4 Max frequency	: 1000 Hz
5 Nozzle diameter	: 1.2 mm
6 Nozzle standoff	: 0.5 mm
7 Focal lens	: 120 mm
8 Focal Spot size	: 180 μ m

Table 2 : Chemical composition of Al7075

Element	Si	Fe	Cu	Mn	Mg	Cr	Zn	Ti	Al
Weight%	0.4	0.5	1.6	0.3	2.5	0.15	5.5	0.2	88.85

Table 3: Control Factors and their levels

S.No	Control Factor	Symbol for coded value	Levels					Units
			-2	-1	1	0	1	
1	Pulse Power	X ₁	210	220	230	240	250	W
2	Pulse Frequency	X ₂	210	220	230	240	250	Hz
3	Assist Gas Pressure	X ₃	8	9	10	11	12	Kg/cm ²
4	Pulse Width	X ₄	0.2	0.3	0.4	0.5	0.6	ms

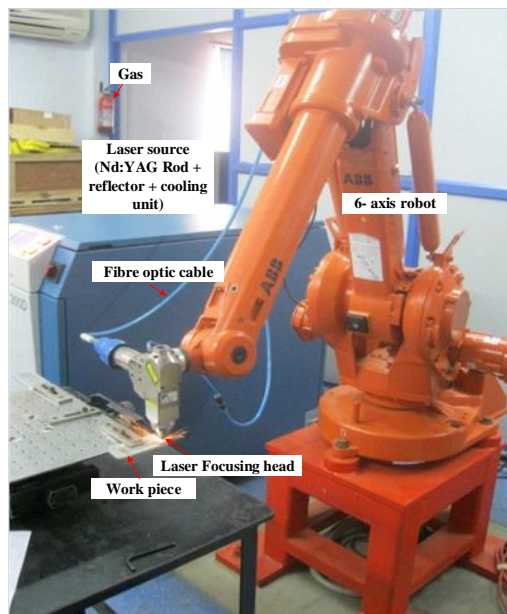


Figure 3: Schematic Representation of Robotic LBC Process

Table 4: Experimental Dataset

NO	X ₁ (W)	X ₂ (Hz)	X ₃ (kg/cm ²)	X ₄ (ms)	Kerf Width (mm)	Kerf Deviation (mm)
1	240	220	11	0.5	0.33000	0.01200
2	220	220	9	0.5	0.30820	0.02100
3	230	230	10	0.4	0.36650	0.01900
4	220	240	11	0.5	0.31299	0.02800
5	220	220	11	0.3	0.32950	0.04100
6	230	230	10	0.4	0.36650	0.01900
7	240	220	9	0.3	0.33900	0.01700
8	240	240	11	0.3	0.36400	0.02870
9	220	240	9	0.3	0.29900	0.01900
10	240	240	9	0.5	0.34050	0.03870
11	220	240	11	0.3	0.32949	0.03200
12	220	240	9	0.5	0.31299	0.02100
13	220	220	9	0.3	0.31285	0.02500
14	230	230	10	0.4	0.36650	0.01900
15	240	240	11	0.5	0.34100	0.02900
16	240	220	9	0.5	0.34500	0.02100
17	230	230	10	0.4	0.36650	0.01900
18	240	240	9	0.3	0.31800	0.03250
19	220	220	11	0.5	0.29900	0.02660
20	240	220	11	0.3	0.35100	0.01570
21	230	230	10	0.4	0.36650	0.01900
22	250	230	10	0.4	0.36650	0.02380
23	230	250	10	0.4	0.31850	0.01900
24	230	230	10	0.2	0.34150	0.02430
25	230	230	12	0.4	0.34900	0.04300
26	230	230	8	0.4	0.32250	0.03360
27	230	230	10	0.4	0.36650	0.01900
28	210	230	10	0.4	0.29830	0.02370
29	230	230	10	0.6	0.32600	0.02200
30	230	210	10	0.4	0.31400	0.01100

Table 5: Analysis of Variance for kerf width

Source	Degrees of freedom (df)	Sum of squares (SS)	Mean square (MS)	F	P-Value
Regression	14	0.0160000	0.001143	75.59	0.000
Linear terms	4	0.0016204	0.000405	26.79	0.000
Square terms	4	0.0026620	0.000666	44.01	0.008
Interaction terms	6	0.0002567	0.000043	2.83	0.000
Residual error	15	0.0002268	0.000015		
Total	29				

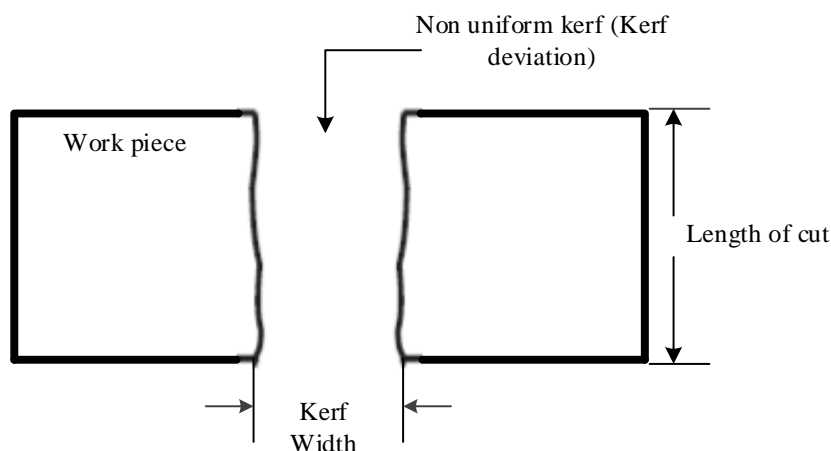


Figure 4: Schematic Representation of kerf width and kerf deviation

Table 6: Analysis of Variance for kerf deviation

Source	Degrees of freedom (df)	Sum of squares (SS)	Mean square (MS)	F	P-Value
Regression	14	0.00179300	0.000128	56.54	0.000
Linear terms	4	0.00006591	0.000016	7.27	0.000
Square terms	4	0.00019000	0.000048	20.97	0.048
Interaction terms	6	0.00012860	0.000021	9.46	0.000
Residual error	15	0.00003398	0.000002		
Total	29				

8.1. Effect of process parameters on kerf width

8.1.1. Direct effects:

Figure 7(a) exhibits that an increase of power lead to an increase in kerf width. The minimum value for the kerf width is obtained for the lowest power, and beyond this value results in an increase in kerf width. An increase of laser power influences to reduction of cut quality, thereupon higher kerf widths result. At higher range if gas pressure is not increased, more molten material is ejected towards the top of the interaction zone and is melting additional material resulting in large kerf. The average cut width increases as the laser cutting energy increases. Low power leads to small thickness of recast layer and additionally causes low kerf width. As shown in Figure 7(b) at low pulse frequency, there is enough time between the pulses for the material to substantially cool down. This helps extinguish the exothermic oxidation reaction thereby reducing the overall process efficiency. Furthermore as the material cools down between pulses at low pulse frequencies, there is greater likelihood of forming dross. The resulting lower average temperature increases the surface tension or viscosity of the molten material making it more difficult to flow out of the reaction zone, thus increasing the kerf width. The average kef width generally increases with increasing the gas pressure as shown in Figure 7(c). The faster the cutting, the smaller the energy density supplied to the material and lesser

time there is for the heat to diffuse sideways and hence the narrower the kerf. Due to small work piece thickness, no significant variation in kerf width is detected. The kerf width varies from lower to higher values as shown in Figure 7(d) due to different material removal mechanisms. At lower levels of pulse width due to lower pulse-to-pulse overlap, individual laser pulses affect the kerf width.

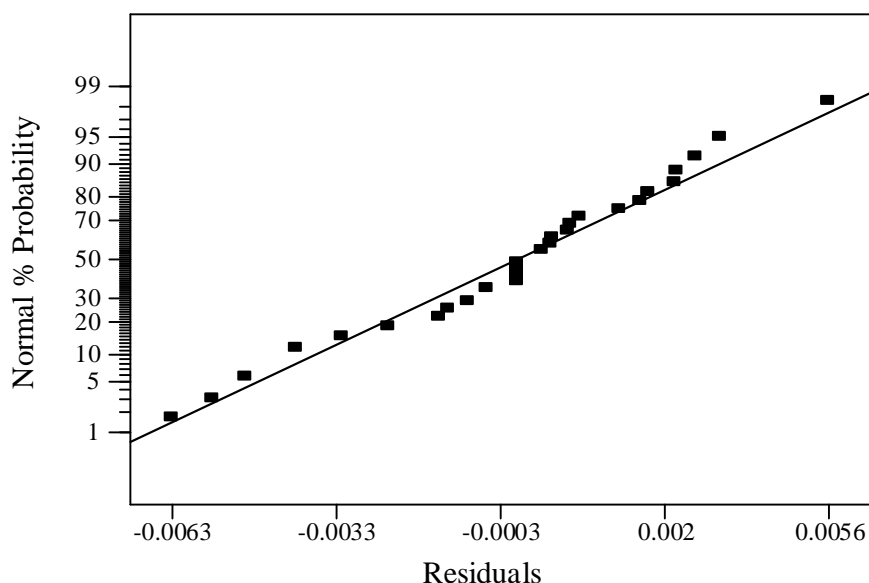


Figure 5: Normal Probability plot for kerf width

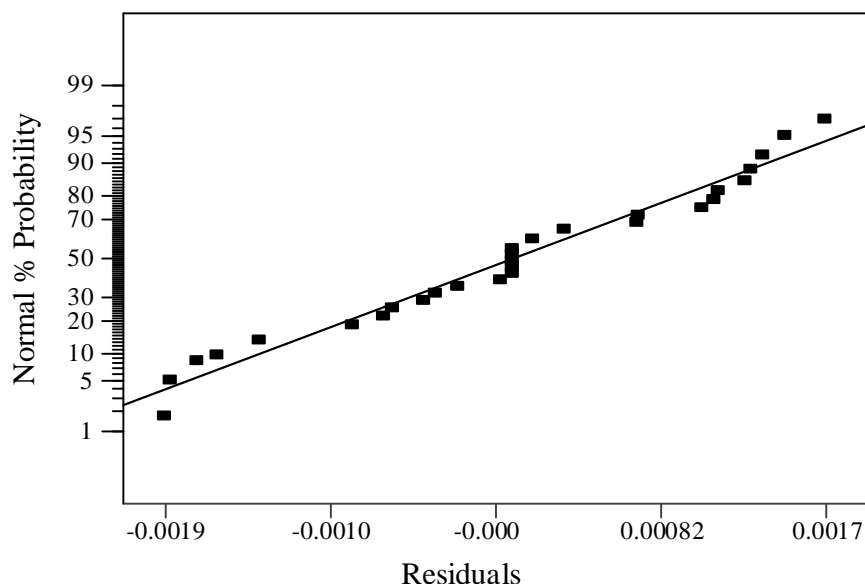


Figure 6: Normal Probability plot for kerf deviation

8.1.2. Surface effects:

Figure 9 shows the 3D surface plots for kerf width. The response surface plot showing the effect of significant parameters (pulse power and pulse frequency) on kerf width has been shown in Figure 9(a) in which the value of assist gas pressure and pulse width remain constant at 10kg/cm² and 0.40 ms. From the figure, it is clear that kerf width increases by increasing the pulse power at lower values of pulse frequencies but at higher values of pulse frequencies, kerf width decreases by increasing pulse frequency. Figure 9(b) exhibits the effects of pulse width and gas pressure on kerf width by keeping laser power and pulse frequency constant at 230W and 230Hz, respectively. From the response graph it has been observed that kerf decreases linearly with the increase in gas pressure at lower value of pulse width. At lower pulse width, small variation has been found in kerf, however very small or negligible changes are found at higher pulse width with the decrease in gas pressure. From the surface plot, it has also been observed that kerf width decreases non-linearly with the increase in pulse width at lower level of gas pressure. With the increase of pulse width, laser will interact with the work piece for a long time with less peak power due to which more thermal energy will be distributed on the top surface resulting in the formation of wide top kerf width. From the surface plot (Figure 9(c)) of kerf width, the effects of pulse frequency and gas pressure at pulse power of 230W and pulse width of 0.6ms has been analyzed. It has been observed from the response graph that the nature of variation of kerf width with applied pulse frequency is almost the same as shown in Figure 9(b). Here, kerf width also decreases linearly with the increase in gas pressure at lower value of pulse frequency.

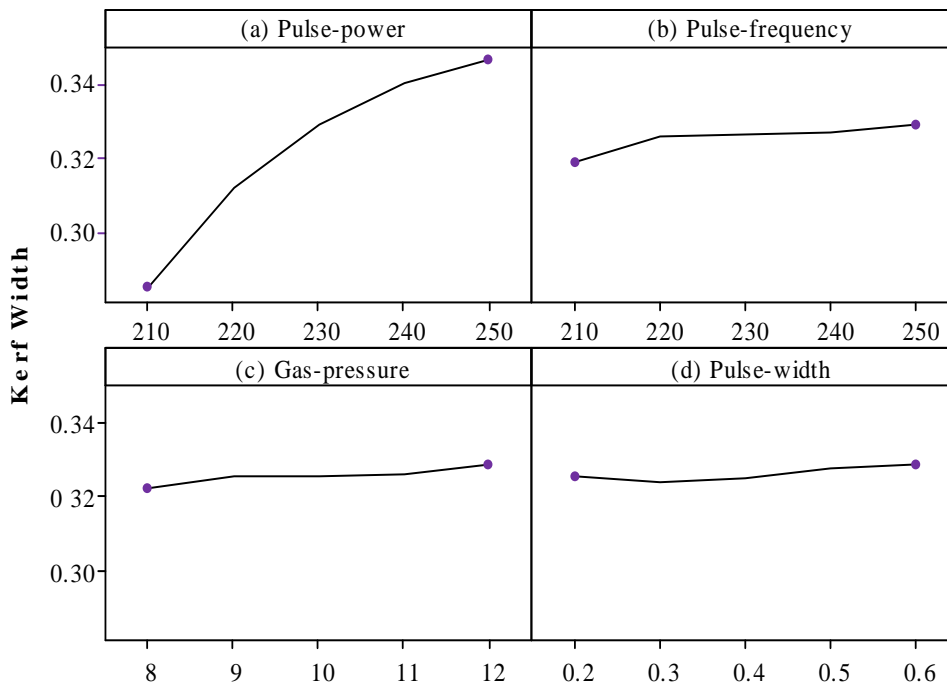


Figure 7: Direct effects of process parameters on kerf width, (a) Pulse-power, (b) Pulse-frequency, (c) Gas-pressure and (d) Pulse-width

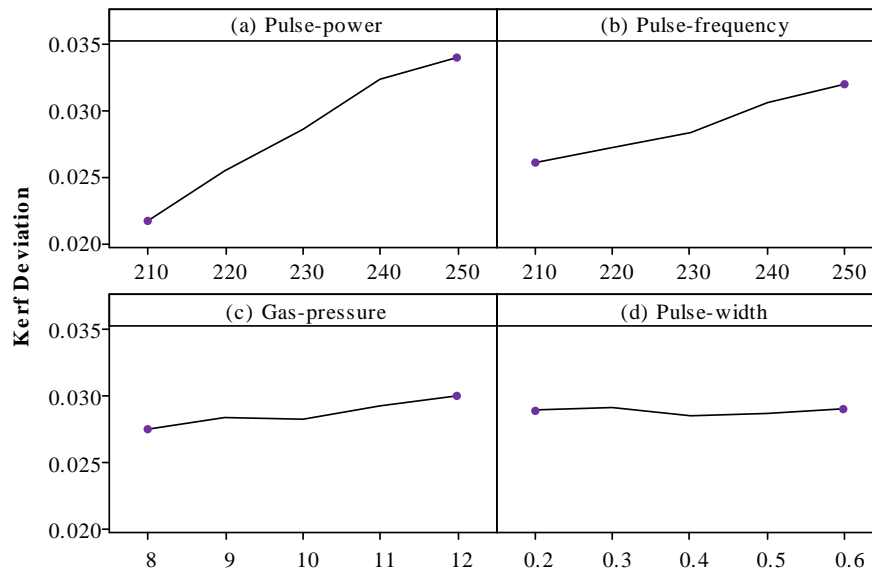


Figure 8: Direct effects of process parameters on kerf deviation, (a) Pulse-power, (b) Pulse-frequency, (c) Gas-pressure and (d) Pulse-width

8.2. Effect of process parameters on kerf deviation

8.2.1. Direct effects:

Figure 8(a) shows that an increase of power lead to an increase in kerf deviation. The minimum value for the kerf deviation is obtained for the lowest power, and exceeding this value results in an increase in kerf deviation. An increase of laser power leads to reduction of cut quality, consequently higher kerf deviation (kerf unevenness) result. At higher range if gas pressure is not increased, more molten material is ejected towards the top of the interaction zone and is melting additional material resulting in large kerf deviation. The average cut width increases as the laser cutting energy increases. Low power leads to small thickness of recast layer and additionally causes low kerf unevenness. As shown in Figure 8(b) at low pulse frequency, there is enough time between the pulses for the material to substantially cool down. This helps extinguish the exothermic oxidation reaction thereby reducing the overall process efficiency. Furthermore, as the material cools down between pulses at low pulse frequencies, there is greater likelihood of forming dross. The resulting lower average temperature increases the surface tension or viscosity of the molten material making it more difficult to flow out of the reaction zone, thus increasing the kerf deviation. The average kef deviation generally increases with increasing the gas pressure as shown in Figure 8(c). The faster the cutting, the smaller the energy density supplied to the material and lesser time there is for the heat to diffuse sideways and hence the narrower the kerf deviation. Due to small work piece thickness, no significant variation in kerf deviation is detected. The kerf deviation varies from lower to higher values as shown in Figure 8(d) due to different material removal mechanisms. At lower levels of pulse width due to lower pulse-to-pulse overlap, individual laser pulses affect the kerf.

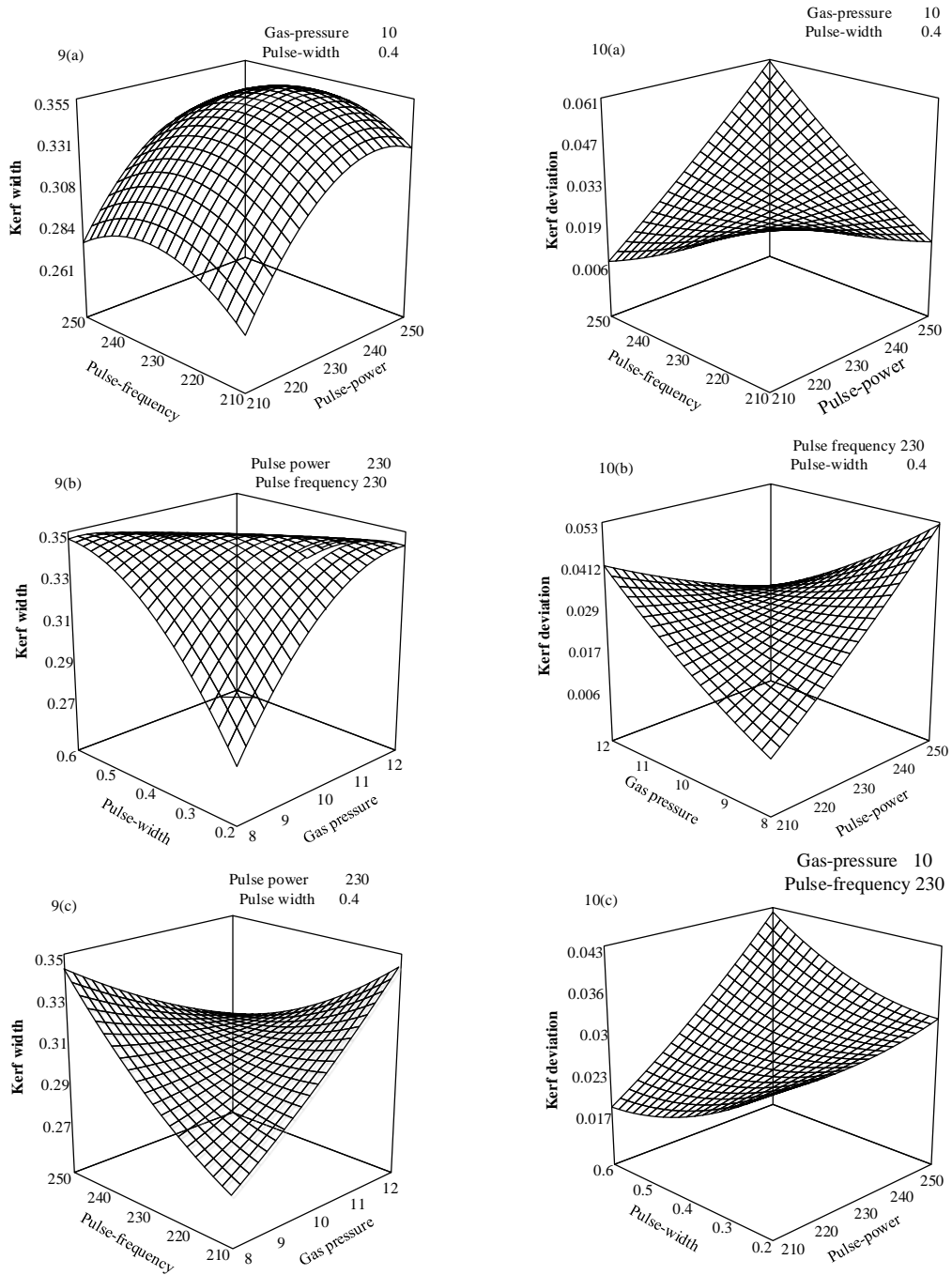


Figure 9(a)-(c): 3D surface plots for kerf width
Figure 10(a)-(c): 3D surface plots for kerf deviation

8.2.2. Surface effects:

Figure 10(a) shows effect of pulse power and pulse frequency on kerf deviation keeping gas pressure and pulse width constant at 10kg/cm^2 and 0.4ms respectively. It is observed that kerf deviation increases with the pulse power significantly irrespective of pulse frequency.

The nature of variation of the unevenness of kerf with applied pulse power is almost similar for the different pulse frequencies and the nature of variation is almost linear. It is due to the fact that energy of laser beam mainly depends on pulse power.

High pulse power generates high thermal energy, as a result top surface of work sample where the laser beam is focused, get melted and vaporized instantly and large volume of material is removed from the top surface during penetration into the remaining thickness, which produces large deviation of kerf.

The low energy of laser beam generates small deviation. From the response plot it has been observed that the kerf deviation almost varies linearly with pulse frequency. At very high pulse frequency, relatively large deviation is observed but at low pulse frequency, low taper is generated.

At very low pulse frequency, the beam energy is slightly high but time between two successive incident beams is more, therefore, material has been removed only from the narrow focusing spot on the top surface of work sample. The effects of pulse power and gas pressure on kerf deviation have been shown in Figure 10(b). Pulse frequency and pulse width are taken as 230Hz and 0.4ms respectively.

The surface plot reflects that gas pressure has linear effect on kerf deviation at different pulse power. At lower level of gas pressure, the variation in kerf deviation with power is much more, but at the higher level of gas pressure, variation in deviation is comparatively less with respect to pulse power. At lower level of power, kerf unevenness is significantly decreasing with the increase in gas pressure.

At low pulse power the amount of heat generation is much lower causing slow rate of material removal. Figure 10(c) exhibits effect of pulse power and pulse width on kerf deviation keeping gas pressure and pulse frequency constant at 0.4 kg/cm^2 and 230Hz , respectively.

At the lower pulse width, variation in kerf deviation is very large with the increase in pulse power, but at the higher pulse width, increases in pulse power results very little variation of kerf deviation. Because at low pulse width high concentrated laser beam energy causes faster rate of penetration compared to high pulse width, as a result less kerf deviation is formed.

It is evident from Figures. 7, 8, 9 and 10 pulse power has profound effect on both the responses among the chosen four control factors.

9. FORMULATION OF COMPOSITE OBJECTIVE FUNCTION OPTIMIZATION USING GA

In the process of optimization, the objective is to minimize kerf width and kerf deviation, which forms the formulation of composite objective function. Mathematical models for kw and kd are represented by Eqns.2 and 3 respectively where X_1 , X_2 , X_3 , and X_4 represents the logarithmic transformations of PP, PF, GP and PW respectively and were given below:

$$\left. \begin{aligned} X_1 &= \frac{\ln(A_1) - \ln(230)}{\ln(250) - \ln(230)} \\ X_2 &= \frac{\ln(A_2) - \ln(230)}{\ln(250) - \ln(230)} \\ X_3 &= \frac{\ln(A_3) - \ln(10)}{\ln(12) - \ln(10)} \\ X_4 &= \frac{\ln(A_4) - \ln(0.4)}{\ln(0.6) - \ln(0.4)} \end{aligned} \right\} \quad (4)$$

The above relations were obtained from the following transformation equation:

$$X_n = \frac{\ln(A_n) - \ln(A_{n0})}{\ln(A_{n1}) - \ln(A_{n0})} \quad (5)$$

where X_n is the coded value of any factor corresponding to its natural value A_n ; A_{n1} is the natural value of the factor at the + level, and A_{n0} is the natural value of the factor corresponding to the base level or zero level. The objective functions are optimized by applying the composite objective function optimization method as follows:

$$\text{Min } Z = \sum_{i=1}^n W_i Y_i / Y_i^* \quad (6)$$

Where Z represents the composite objective function to be minimized, Y_i states the value of the response variable i , Y_i^* and W_i represent the average value and weight factor (0.5) of the response variable i and n represents the number of responses. The composite objective function is optimized subject to the feasible bounds of the control variables. Table 7 exhibits the feasible bounds for each variable.

Variable	Lower limit	Upper limit
Pulse-power (X_1)	210	250
Pulse-Frequency (X_2)	210	250
Assist gas Pressure (X_3)	8	12
Pulse-width (X_4)	0.2	0.6

10. RESULTS AND DISCUSSION

A Pentium IV processor using Microsoft VC++ programming language on a Windows XP platform was availed to run the source code of the contemplated optimization algorithm. Table 8 lists the GA control parameters used for implementation of the algorithm. The population size, crossover and mutation probability and number of generations are important factors for better performance of the algorithm. The large size of the population results the better searching of the solution space and reduces the chance of getting poor solution [23]. The algorithm constituted the convergence graph of the composite objective function with acceptable distinctiveness of the solutions, as shown in Figure 11.

Population size	100
Number of generations	500
Crossover Probability	0.85
Mutation Probability	0.01

The optimal machining parameters found after the implementation of the algorithm are given in Table 9.

PP(W)	PF (Hz)	GP(Kg/cm ²)	PW(ms)	Fitness value
250	210	11.29	0.6	0.20345

11. CONCLUSIONS

Laser Beam Cutting process (LBC) is substantial and successfully used nontraditional machining technology overwhelmingly used for the cutting of conductive and nonconductive difficult-to-cut advanced engineering materials yielding tremendous flexibility and quality. Yet, the assortment of pertinent combination of input parameters in LBC is exigent as the approach necessitates a considerable number of control parameters. The enduring analysis contemplated a methodology for LBC based on the RSM and GA to evaluate the optimal machining parameters and to accomplish magnificent production machined components. RSM is a powerful mathematical model widely used to examine and optimize the operational variables for experiment designing and model developing whereas GA is cost effective soft computing technique for optimizing machining operations.

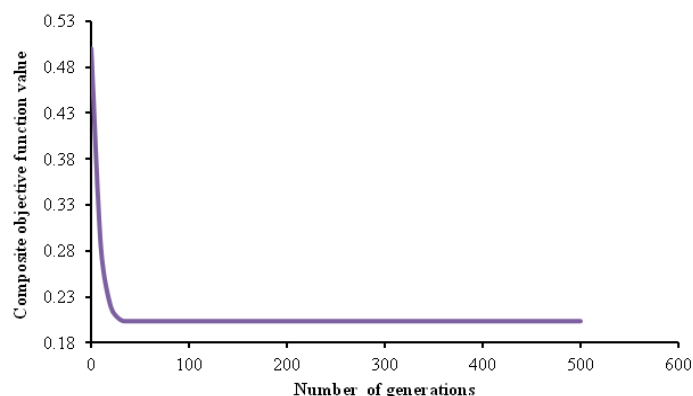


Figure 11: Convergence graph of GA

In this analysis, the performances of LBC, namely kw and kd were enumerated. From the experimental details, RSM was used to model the mathematical equations for the selected performance responses. The central composite rotatable factorial design was used to diminish the number of experimental values. Subsequently, the validated mathematical models of RSM were used by GA to find the composite objective function values for minimization of kerf width and kerf deviation so as to empower a manufacturing engineer to determine appropriate optimal solutions according to the specific requisitions.

References

- 1) Steen, W. M. 1998. *Laser material Processing. 2nd Edition*. Springer, London.
- 2) Radovanovic, M., and Madic, M. 2011. Experimental Investigations of CO₂ Laser Cut Quality: A Review, *Non-conventional Technologies Review*, 15(4), pp. 35-42.
- 3) Harrington, W. C. 1993. Mechanical Properties of Metallurgical composites. (edited by S. Ochiai), *Marcel Dekker Inc., NY*, pp. 759.
- 4) Hung, N. P., Ng, K. J., and Low, K.W. 1996. Review on conventional machining of metal matrix composites. *Proceedings Engineering Systems Design and Analysis*, 75(3), pp. 75-80.
- 5) Mohan, B., Rajadurai, A., and Satyanarayana, K. G. 2002. Effect of SiC and rotation of electrode on electric discharge machining of Al-SiC composite. *Journal of Materials Processing Technology*, 124(3), pp. 297-304.
- 6) Schreck, S., and Zum Gahr, K. H. 2005. Laser-assisted structuring of ceramic and steel surfaces for improving tribological properties [J]. *Appl. Surf. Sci*, 247(1), pp. 616-622.
- 7) Cenna, A. A., and Mathew, P. 2002. Analysis and prediction of laser cutting parameters of fibre reinforced plastics (FRP) composite materials. *International Journal of Machine Tools & Manufacture*, 42(1), pp. 105-113.
- 8) Dillio, A., Tagliaferri, V., and Veniali, F. 1990. Machining parameters and cut quality in laser cutting of fibre reinforced plastics. *Materials and Manufacturing Processes*, 5(4), pp. 591-608.
- 9) Luxon, J. T., and Parker, D. E. 1985. *Industrial Lasers and their Applications*. Prentice Hall, London.
- 10) Thawari, G., Sarin Sundar, J. K., Sundararajan, G., and Joshi, S.V. 2005. Influence of process parameters during pulsed Nd: YAG laser cutting of nickel-base super alloys. *J Mater Process Tech*, 170(1), pp. 229-239.

- 11) Quintero, F., Pou, J., Lusquinos, F., Boutinguiza, M., Soto, R., and Perez-Amor, M. 2004. Quantitative evaluation of the quality of the cuts performed on Mullite-alumina by Nd: YAG laser. *Optic Laser Eng*, 42(3), pp. 327-340.
- 12) Ghany, K. A., and Newishy, M. 2005. Cutting of 1.2 mm thick austenitic stainless steel sheet using pulsed and CW Nd: YAG laser. *J. Mater. Process. Technol*, 168(3), pp. 438-447.
- 13) Dubey, A. K., and Yadava, V. 2008. Multi-objective optimization of laser beam cutting process. *Optic Laser Tech*, 40(3), pp. 562–570
- 14) Avanish Kumar, D., and Vinod, Y. 2008. Optimization of kerf quality during pulsed laser cutting of aluminium alloy sheet. *J Mater Process Technol*, 204(11), pp. 412–418.
- 15) Raghavendra, R., and Vinod, Y. 2009. Multi-objective optimization of Nd: YAG laser cutting of thin super alloy sheet using grey relational analysis with entropy measurement. *Optics and Laser Technology*, 41(8), pp. 922-930.
- 16) Avanish Kumar, D., and Vinod, Y. 2008. Multi-objective optimization of Nd: YAG laser cutting of nickel-based super alloy sheet using orthogonal array with principal component analysis. *Optics and Lasers in Engineering*, 46(2), pp. 124-132.
- 17) Amit, S., Vinod, Y., and Raghavendra, R. 2010. Optimization of kerf quality characteristics during Nd: YAG laser cutting of nickel based super alloy sheet for straight and curved cut profiles. *Optics and Lasers in Engineering*, 11(4), pp. 915-925.
- 18) Sivarao., Peter, B., Tayeb, N. S. M., and Vengkatesh, V. C. 2009. ANFIS Modeling of Laser Machining Responses by Specially Developed Graphical User Interface. *International Journal of Mechanical & Mechatronics Engineering*, 9(9), pp. 181-189.
- 19) Kaebernick, H., Bicleanu, D., and Brandt, M. 1999. Theoretical and experimental investigation of pulsed laser cutting – *CIRP Annals-Manufacturing Technology*, 48(1), pp. 163-166.
- 20) Yue, T. M., and Lau, W.S. 1996. Pulsed Nd: YAG Laser Cutting of Al/Li/SiC Metal Matrix Composites. *Materials and Manufacturing Processes*, 11(1), pp. 17–29.
- 21) Jain, N. K., Jain, V. K., and Jha, S. 2007. Parametric optimization of advanced fine-finishing processes. *Int. J. Adv Manuf Technol*, 34(11), pp. 1191-1213.
- 22) Sardinas, R. Q., Santana, M. R., and Brindis, E. A. 2006. Genetic algorithm based multi objective optimization of cutting parameters in turning processes. *Engng Applic. Artif. Intell* 19, pp. 127-133.
- 23) Maghsoud, A., Amir, N., and Komeil, G. 2008. Response surface Methodology and genetic algorithm in Optimization of Cement Clinkering Process. *Journal of Applied Sciences*, 8(15), pp. 2732-2738.
- 24) Box, G. E. P., and Wilson, K. B. 1951. Experimental attainment of optimum conditions. *J R Stat Soc [Ser A]* 13, pp. 1–45.
- 25) Hill, W. J., and Hunter, W.G.1966. A review of response surface methodology: a literature review. *Technometrics* 8, pp. 571–590.
- 26) Montgomery, D.C. 2001. Design and analysis of experiments. Wiley, Hoboken.
- 27) Holland, J.H. 1975. Adaptation in Natural and Artificial Systems. University of Michigan Press, Ann Arbor.
- 28) Design Expert, 7.1.3v. 2006. Stat-Ease Inc., 2021 E. Hennepin venue, Suite 480, Minneapolis.
- 29) Montgomery, D. C., Peck, E. A., and Vining, G. G. 2003. Introduction to linear regression analysis, 3rd edn. Wiley, New York.